Dual species dynamic transcripts reveal the interaction mechanisms between *Chrysanthemum morifolium and Alternaria alternata*

Lina Liu
Nanjing Agricultural University
Fadi Chen
Nanjing Agricultural University
Sumei Chen
Nanjing Agricultural University
Weimin Fang
Nanjing Agricultural University
Ye Liu (liuye@njau.edu.cn)
Nanjing Agricultural University https://orcid.org/0000-0002-9556-0814
Zhiyong Guan
Nanjing Agricultural University

Research article

Keywords: dual RNA-seq, Chrysanthemum morifolium, Alternaria alternata, plant-pathogen interaction, WGCNA

Posted Date: August 21st, 2020

DOI: https://doi.org/10.21203/rs.3.rs-60096/v1

Version of Record: A version of this preprint was published at BMC Genomics on July 9th, 2021. See the published version at https://doi.org/10.1186/s12864-021-07709-9.

Abstract

Background

Chrysanthemum (*C. morifolium*) black spot disease caused by *Alternaria alternata* is one of the plant's most destructive diseases. Dual RNA-seq was performed to simultaneously assess their transcriptomes to analyze the potential interaction mechanism between the two species, i.e., host and pathogen.

Results

C. morifolium and *A. alternata* were subjected to dual RNA-seq at 1, 12, and 24 hours after inoculation, and differential expression genes (DEGs) in both species were identified. This analysis confirmed 153,532 DEGs in chrysanthemum and 14,932 DEGs in *A. alternata*, that were involved in plant-fungal interactions and phytohormone signaling. Fungal DEGs such as toxin synthesis related enzyme and cell wall degrading enzyme genes played important roles during chrysanthemum infecton. Moreover, a series of key genes highly correlated with the early, middle, or late infection stage was identified, together with the regulatory network of key genes annotated in PRG or PPI databases. Highly correlated genes were identified at the late infection stage, expanding our understanding of the interplay between *C. morifolium* and *A. alternata*. Additionally, six DEGs each from chrysanthemum and *A. alternata* were selected for qRT-PCR assays to validate the RNA-seq output.

Conclusions

Collectively, data obtained in this study enriches the resources available for research into the interactions that exist between chrysanthemum and *A. alternata*, thereby providing a theoretical basis for the development of new chrysanthemum varieties with resistance to pathogen.

Background

Chrysanthemum, one of the most commercially important ornamental crops worldwide, is widely used as cut flowers, potted plants, and in landscaping. It carries a long history of cultivation, high ornamental, edible, and medicinal value [1]. Chrysanthemum are susceptible to pathogen invasion during cultivation, especially when grown on a large scale. Alternaria leaf spot is a major disease of chrysanthemum that readily occurs at high temperatures and during continuous rainy seasons. Following a symptomless early infection stage, small round black spots form at the *A. alternata* invasion site, which eventually expand into round, round-like, or irregular spots covered with a dark mildew layer [2]. Currently, the main method of *A. alternata* control in chrysanthemum is via fungicide application. However, a prolonged use of these chemicals can result in pathogen resistance and environmental pollution. Thus, a better understanding of the defense mechanisms employed by chrysanthemum in response to *A. alternata* will help design new and safer control strategies, as well as develop resistant cultivars. By performing dual RNA-seq analysis

on chrysanthemum and *A. alternata* simultaneously, we can understand changes in transcriptional expression related to chrysanthemum defense against *A. alternata*. Furthermore, we can determine which *A. alternata* genes interact with chrysanthemum and analyze the molecular response of *A. alternata*-infected plants.

In response to external biotic stress, plants induce a range of immune responses, including physical barriers (e.g., keratin, wax, lignin, and special stomatal structures) [3], chemical barriers (e.g., secondary metabolites with antibacterial properties) [4] and molecular responses (e.g., hypersensitive response, production of reactive oxygen species, and expression of pathogen-related genes) [5]. High-throughput sequencing technology, especially RNA-seq, tracks more precise molecular changes in plants under biotic and abiotic stress. This method has been widely applied in research on plant-pathogen interactions in agricultural crops, including in apple (*Malus × domestica*) [6], citrus [7], gape (*Vitis vinifera*) [8], pear (*Pyrus pyrifolia*) [9], soybean [10], and tomato (*Solanum lycopersicum*) [11]. The studies above were limited to a unilateral transcription analysis of plants under pathogenic stress. More recently, dual RNA-seq has become a powerful tool for comprehensively understanding host-pathogen interactions in vivo [12], that can simultaneously capture pathogen-specific transcripts during the infection process, provide a more complete view of interactions [13], reveal biosynthetic and metabolic pathways of crosstalk among participants, and specifically determine the dynamic expression profile of genes associated with host-pathogen interactions [14]. To date, the mutual in vivo attack and counterattack response between chrysanthemum and *A. alternata* is poorly understood. The present study aimed to investigate *C. morifolium* infected with *A. alternata* using dual RNA-seq analysis.

RNA-seq libraries were constructed and identified DEGs were further analyzed. The expression of fungal genes was also investigated at three infection stages, in an attempt to discover genes that could potentially threaten the cultivation of chrysanthemum. Through dual RNA-seq, we hoped to gain insights into the interaction between *C. morifolium* and *A. alternata* and to investigate the potential pathogenesis of *A. alternata*, as well as the defense mechanism of *C. morifolium*, which would benefit in inhibiting fungal pathogenicity or breed resistant chrysanthemum cultivars.

Results

Statistical analysis of RNA-seq results

A. alternata morphology symptom changes in inoculated chrysanthemum leaves, and the dual RNA-seq analysis process are shown in Figure 1. Three samples sets, each with three biological replicates, were subjected to dual RNA-seq at each time point, and 27 cDNA libraries were generated: CK1h_1, CK1h_2, CK1h_3, CK12h_1, CK12h_2, CK12h_3, CK24h_1, CK24h_2, CK24h_3, Aa1h_1, Aa1h_2, Aa1h_3, Aa12h_1, Aa12h_2, Aa12h_3, Aa24h_1, Aa24h_2, Aa24h_3, In1h_1, In1h_2, In1h_3, In12h_1, In12h_2, In12h_3, In24h_1, In24h_2, In24h_3. Table S2 shows the summary statistics of original reads and filtered clean reads of three replicates at each time point, for chrysanthemum. Inoculated and control samples generated on a average 41.20 Mb and 108.76 Mb clean reads, respectively, all with 100% read ratio.

Furthermore, at each tome point, inoculated and control samples contained average 4.12 Gb clean bases and 10.88 Gb of clean bases, respectively. Table S3 lists the summary statistics of original reads and filtered clean reads obtained from three replicates at each time point, for *A. alternata*. The average clean reads of the inoculated and control samples generated on average 108.93 Mb and 108.64 Mb clean reads, respectively, with a read ratio ≥ 92.54%. Moreover, at each time point, inoculated and control samples contained an average of 10.89 Gb and 10.86 Gb of clean bases, respectively.

The clustered quality indicators of chrysanthemum are shown in Table S4. Infected and control chrysanthemum samples contained an average of 35,843 and 54,560 unigenes, respectively. The total length of chrysanthemum library transcripts was ≥ 14,571,366, the average length of the library was ≥ 642, N50, N70, and N90 ≥ 865, 556, 296, respectively. The GC ratio was ≥ 40.45%. Comparison of all unigenes to the seven major functional databases for annotation, generated the following numerical data: 89,889 (NR: 72.62%), 55,679 (NT: 44.98%), 61,156 (SwissProt: 49.41%), 64,694 (KOG: 52.26%), 64,705 (KEGG: 52.27%), 68,727 (GO: 55.52%), and 60,671 (Pfam: 49.01%) (Table S5). The average total mapping percentage of *A. alternata* at each time point was higher than 56.9%, and that of the control group was higher than 86.53% (Table S6).

Identification of DEGs

Comparison of gene expression between the ‘In’ and ‘CK’ sample series detected27,029 DEGs (21,216 up-regulated and 5,813 down-regulated) for In1h vs. CK1h, 76,932 DEGs (18,446 up-regulated and 58,486 down-regulated) for In12h vs. CK12h, and 49,571 DEGs (29,642 up-regulated and 19,929 down-regulated) for In24h vs. CK24h (Figure 2A). Illustration of these results as a Venn diagram clearly showed that both unique and shared DEGs were identified between, and among times points (Figure 2B). For example, 18,318, 20,696, and 37,618 shared DEGs were detected in the 1 HPI vs. 12 HPI, 1 HPI vs. 24 HPI, and 12 HPI vs. 24 HPI comparisons, respectively, while 15,960 DEGs were found in the 1 HPI vs. 12 HPI vs. 24 HPI comparison (Figure 2B). These results suggested that, as pathogen infection progressed, an increasing number of genes became involved in defense responses.

The degree of GO term enrichment was similar for the three inoculation time points, and DEGs were divided into 54 functional categories according to biological processes (25), cellular components (16), and molecular functions (13). The most significantly enriched biological processes were “regulation of transcription, DNA-templated”, “carbohydrate metabolic process”, and “translation”; the most significantly enriched cellular components were “cytoplasm”, “ribosome”, and “chloroplast”, while “protein serine/threonine kinase activity”, “nucleic acid binding” and “oxidoreductase activity” occupied the important positions in molecular functions (Figure 2D). Moreover, a total of 30 KEGG pathways were significantly enriched at 1, 12, and 24 HPI, each with a varying number of DEGs (Table S7). Maps with the highest DEG representation were those for ‘plant-pathogen interactions’ (ko 04626), followed by those for ‘plant hormone signal transduction’ (ko 04075), ‘MAPK signaling pathway-plant’ (ko 04016), ‘carbon metabolism’ (ko 01200) ‘protein processing in endoplasmic reticulum’ (ko 04141) and ‘biosynthesis of amino acids’ (ko01230). The above results indicated that chrysanthemum infected with *A. alternata*

involved a series of defense strategies interacting with multiple pathways to jointly regulate and respond to pathogenic stress. These strategies dominated at different infection stages.

Gene expression comparison between the 'In' and 'Aa' sample series found 4,027 DEGs (2,729 up-regulated and 1,298 down-regulated) for In1h vs. Aa1h, 5364 DEGs (3697 up-regulated and 1667 down-regulated) for In12h vs. Aa12h, and 5,541 DEGs (3572 up-regulated and 1969 down-regulated) for In24h vs. Aa24h (Figure 2A). Moreover, analysis of Venn diagram showed 3,066, 2.881, and 4,176 shared DEGs in the 1 HPI vs. 12 HPI, 1 HPI vs. 24 HPI, 12 HPI vs. 24 HPI, and 1 HPI vs. 12 HPI vs. 24 HPI comparison (Figure 2C).

The degree of GO term enrichment was similar among the three stages of *A. alternata* infection and DEGs were divided into 38 functional categories, according to biological processes (16), cellular components (12), and molecular functions (10). "Metabolic process", "organic substance metabolic process" and "cellular process" were the most significantly enriched biological processes; the most significantly enriched cellular components were detected in "cell", "cell part", and "intracellular"; while "hydrolase activity", "organic cyclic compound binding" and "heterocyclic compound binding" occupied the important positions in molecular functions (Figure 2E). Moreover, a total of 20 KEGG pathways were significantly enriched at the three stages, but with varying numbers of DEGs (Table S8). Maps with the highest DEGs representation were for 'biosynthesis of antibiotics' (ko 01130), followed by 'MAPK signaling pathway-yeast' (ko 04011), 'amino sugar and nucleotide sugar metabolism' (ko 00520) and 'glycine, serine and threonine metabolism' (ko 00260). The above results indicated that *A. alternata* induced a variety of metabolic activities during chrysanthemum infection, that generated energy and toxic metabolites to attack host cells. These metabolic processes played a key role in the interaction between chrysanthemum and *A. alternata*.

DEGs involved in phytohormone signaling

Phytohormones, such as salicylic acid (SA), ethylene (ET), jasmonic acid (JA), brassionosteroid (BR), auxin (AUX), and abscisic acid (ABA), are widely involved and play critical regulatory roles in plant-pathogen interactions [15]. The related DEGs of several hormone signaling pathways in l infected chrysanthemum leaves were analyzed. Several DEGs involved in SA biosynthesis and signaling were differentially expressed, e.g., three DEGs of NPR1 (non-expressors of disease-related genes) and TGA (TGACG motif binding factor) were down-regulated at 1HPI but significantly up-regulated at 24 HPI; two DEGs related to PR1 (proteins related to disease-course) were up-regulated at 1 HPI and one of them was up-regulated at 24 HPI. All DEGs from JAZ were up-regulated during the whole process, and those MYC2 homologous were significantly up-regulated at 24 HPI. Several genes known to be ET-responsive were up-regulated, including EBF 1/2 (F-box protein 1/2 bound to EIN3) at 24 HPI, EIN3 (ethylene-insensitive 3) at 1 HPI and 24 HPI, and ERF1/2 (ethylene response factor 1/2) which exhibited change by a higher multiple. Most DEGs in AUX signaling, such as AUX / IAA (auxin / indole-3-acetic acid), SAUR (small auxin-up RNA) and auxin-responsive GH3 (Gretchen Hagen3 gene) also showed notably up-regulated expression. Previous studies have also shown that BRs comprise a unique class of growth-promoting

steroid hormones, known to be key regulators of plant immunity [16]. DEGs encoding BR signaling cascades included BAK1 (BRI-related receptor kinase 1), BSK (brassinosteroid steroid signal transduction kinase), TCH4 (xyloglucan endotransglucosylase transglucosylase, also named Touch 4) and BZR1/2 (an anti-azole transcription factor). Except for DEGs encoding BZR1/2, that responded to *A. alternata* at 1 HPI, but were down-regulated by a high multiple (7) at 12HPI, the remaining DEGs belonging to the BR signaling cascades, expression level gradually increased at three infection stages. Finally, DGEs involved in the ABA signaling pathway, such as PYR/PYL (pyrabactin resistance1/PYR1-like), PP2C (protein phosphatase 2C), and SnRK2 (sucrose non-fermenting 1-related protein kinase2), were all up-regulated at 24 HPI; ABF (ABA binding factor) was up-regulated at 1 HPI and 24 HPI, but down-regulated at 12 HPI, similar to BZR1/2. The schematic diagram of the relevant hormone pathways is shown in Figure 3A.

DEGs involved in plant-fungal interaction

During biotic stress, chrysanthemum DEGs encoding CDPK (calcium-dependent protein kinase) and Rbohs (respiratory explosive oxidase homologs) were significantly up-regulated over time and were involved in hypersensitive reaction (hereafter named HR) and cell wall reinforcement. DEGs encoding PR-proteins, such as chitinase (CHI, PR3), were generally up-regulated, while the DEGs encoding b-1,3-glucanase (PR2) were specially down-regulated at 1 HPI, but significantly up-regulated at 12 HPI, with a high multiple (> 6) notably induced at 24 HPI. In addition, most DEGs encoding potential CNGCs (cyclic nucleotide gated channels) were up-regulated at 24 HPI, and those encoding CaM/CMLs (crassulacean acid metabolism/calmodulin-like protein) showed similar trends. Furthermore, several downstream defense-related PR proteins, such as PR9 (peroxidase), PR10 (ribonuclease), and PR14 (lipid-transfer protein), were induced and significantly up-regulated at all three time points (Figure 3B).

DEGs related to virulence in *A. alternata*

Alternaria spp. produce a variety of secondary metabolites during the pathogenic process, and more than 70 compounds with significant toxicity have been isolated [17], with important roles in fungal virulence. Most of these toxins are versatile compounds of polyketides and non-ribosomal peptides, which are usually generated by non-ribosomal peptide synthase (NRPS) and polyketide synthase (PKS), respectively [18]. We identified three NRPS genes and seven PKS genes in *A. alternata*, all showing up-regulated expression at the three inoculation stages. DEGs of NRPS (CC77DRAFT_1065195) presented a significantly higher multiple (> 6) at 24 HPI (Figure 4). Previous study have shown that *pksJ* and *pksH* were correlated with the production of alternariol (AOH) and alternariol-9-methyl ether (AME) [19]. We also identified the *pksJ* homolog (*CC77DRAFT_1058721*) and *pksH homolog* (*CC77DRAFT_976935*), both up-regulated during *A. alternata* infection.

Furthermore, fungal cell wall degrading enzymes (CAZymes) can promote degradation of the plant cell wall, penetration into the host tissue, and adhesion layer formation [20]. CAZymes consist of four functional classes: glycoside hydrolases (GHs), glycosyl transferases (GTs), polysaccharide lyases (PLs), and carbohydrate esterases (CEs), classified according to their catalytic modules or functional domains [20]. Expression levels were also investigated during the interaction between *A. alternata* and

chrysanthemum. There were thirteen DEGs of GHs, with most of them significantly up-regulated at the three time points; two DEGs of GTs, one up-regulated and the other down-regulated. Only one DEG of PLs was found, and its expression showed an obviously upward trend. Similar to PLs, only one CE displayed higher expression (Figure 4).

Weighted gene co-expression network analysis (WGCNA)

Weighted gene co-expression network analysis (WGCNA) was carried out to identify genes related to phenotypes and investigated the co-expression networks to elucidate the interaction network between *C. morifolium* and *A. Alternata*. Ultimately, 17 and 29 gene co-expression modules were discovered in in *C. morifolium* and *A. alternata*, respectively, shown in Figure 5A and B.

Genes from the 'Cm_brown', 'Cm_midnightblue', 'Cm_salmon', 'Cm_greenyellow', 'Cm_lightcyan', 'Aa_magenta', 'Aa_yellow', 'Aa_brown', 'Aa_skyblue' and 'Aa_black' modules were highly correlated with the traits observed at the three infection stages (Figure 5A, B). KEGG annotation analyses were performed to further explore what pathways the genes from the modules above were involved in. Plant cell walls can act as a natural physical barrier against pathogens [20]. The cuticle is the first layer of the cell wall that prevents pathogens from invading the cells [21], and usually consists of a horny and a waxy protective film. Its biosynthesis involves several genes, including wax-ester synthase/diacylglycerol O-acyltransferase (WSD) [22], and fatty acid omega-hydroxy dehydrogenase (HTH) [23]. In the 'Cm_turquoise' module, WSD and HTH homologs in *C. morifolium* were significantly up-regulated, and several of these gene homologs (e.g., *Unigene36512_All*, *Unigene36513_All*, and *CL1059.Contig1_All*) displayed an expression fold-change > 10 (Figure S1). The above analysis showed that the cuticle played a positive role in the chrysanthemum defense against *A. alternata*. As reported, pectin lyase, pectate lyase, and xylanase can break down the pectin and xylans present in the plant cell wall. In the 'Aa_black' and 'Aa_green' modules, lyase homologs (e.g., *CC77DRAFT_1043109*, *CC77DRAFT_1048882*, and *CC77DRAFT_167134*) exhibited a high expression level in *A. alternata* during infection (Figure S1).

Highly correlated modules and key genes identification

The relationship between module and trait allowed us to evaluate the correlation coefficient between modules from *C. morifolium* and *A. alternata*. A network of *C. morifolium* and *A. alternata* modules are shown in Figure 6A, and highly correlated modules ($r \geq 0.8$ and p-value < 0.05) are linked by a line (Figure 6A). In the early infection stage, three *C. morifolium* gene modules ('Cm_brown', 'Cm_midnightblue', and 'Cm_salmon',) and five *A. alternata* modules ('Aa_magenta', 'Aa_yellow', 'Aa_brown', 'Aa_darkorange', and 'Aa_pink') were highly correlated; in the middle infection stage, one *C. morifolium* gene modules ('Cm_greenyellow') and three *A. alternata* modules ('Aa_royalblue', 'Aa_black', and 'Aa_green') were highly correlated; in the late infection stage, two *C. morifolium* gene modules ('Cm_turquoise' and 'Cm_lightcyan') and four *A. alternata* modules ('Aa_steelblue', 'Aa_grey60', 'Aa_black', and 'Aa_green') were highly correlated (Figure 6B). Gene significance (value ≥ 0.8) and connectivity (top 20%) were used together to identify key genes in each of the modules above (Figure 6C, D).

Based on gene transcription levels, we performed correlation coefficient analyses between genes from highly correlated modules in *C. morifolium* and *A. alternata* to identify the interplay genes. From modules that highly correlated with the late infection stage, a number of genes were identified and a network of highly correlated genes ($r \geq 0.8$ and p-value < 0.05) were linked by a line, as shown in Figure 7A. Most of these genes were up-regulated with the spread of *A. alternata* (Figure 7B, C, D, E).

Regulatory network of key genes annotated in PPI and PRG databases

The Plant Resistance Genes database (PRGdb; http://prgdb.org) is a bioinformatics platform for plant resistance gene analysis [24]. The pathogen–host interactions database (PHI-base: www.phi-base.org) contains molecular and biological information on genes which have been proven to affect the outcome of host-pathogen interactions [25]. Key genes from the highly correlated modules were examined for further analyses. Seventy-five key genes from *A. alternata* were annotated by PHI-base and twelve key genes were annotated by PRGdb. The regulatory network of these eighty-seven key genes are shown in Figure 8. Notably, two RGA1-like disease resistance protein homologs (*CL2806.Contig1_All* and *CL2806.Contig4_All*) were identified in the late infection stage. Two transcription factors (*CL14283.Contig1_All* and *Unigene25854_All*) were also identified and may play important roles in response to *A. alternata* infection in *C. morifolium* (Figure 8). Additionally, ACL2 homolog (*CC77DRAFT_784023*), ACL1 homolog (*CC77DRAFT_986135*), and BUF1 homolog (*CC77DRAFT_528893*) were identified, which were predicted to influence the virulence of *A. alternata* (Figure 8).

Validation of RNA-seq data by qRT-PCR

To confirm the reliability of the generated dual RNA-seq data, the expression of 12 DEGs were analyzed using qRT-PCR assays, of which six were derived from chrysanthemum, (*CL11098.Contig2_All*, *CL1653.Contig1_All*, *CL5572.Contig1_All*, *Unigene47090_All*, *CL3907.Contig2_All* and *CL11265.Contig3_All*); Figure 9A), and six were from *A. alternata* (*CC77DRAFT_945175*, *CC77DRAFT_1044312*, *CC77DRAFT_1036704*, *CC77DRAFT_598231*, *CC77DRAFT_779096* and *CC77DRAFT_950634*; Figure 9B). qRT-PCR results and RNA-seq data showed similar up-regulation or down-regulation expression patterns. The correlation coefficients between qRT-PCR and RNA-seq of the 12 DEGs were all ≥ 0.85. Minor discrepancies regarding the expression levels might suggest a difference in sensitivity between the two methods. These results highlighted the reliability of the RNA-seq data.

Discussion

Dual RNA-seq of chrysanthemum leaves infected with *A. alternata* was performed to detect the occurrence of any dynamic changes in the plant tissue, which would provide a broader understanding of the mechanism of host-pathogen interaction between the two species. This study compared the gene expression of *A. alternata*, chrysanthemum leaves and chrysanthemum leaves infected with *A. alternata* at three infection stages, i.e., the early (no lesion formation), middle (lesion formation) and late (lesion expansion) infection stage. A total of 153,532 and 14,932 DEGs were identified in chrysanthemum and *A.*

alternata, respectively. The analysis of these DEGs focused on induced pathways in chrysanthemum or *A. alternata* during infection.

A large number of chrysanthemum DEGs of chrysanthemum were enriched in the "Plant-pathogen interaction" pathway. DEGs encoding CDPK and Rboh homologs were also identified, that were accompanied by ROS accumulation during infection, resulting in HR and cell wall enhancement. Several enzyme systems had been reported to characterize oxidative bursts of HR. For instance, ascorbic acid (ASC) can act in coordination with glutathione (GSH) and other important enzymatic antioxidants in the AsA-GSH cycle to provide an appropriate redox environment required to regulate various defense pathways, such as the expression of defense genes through activation of the NPR1 regulatory transcription factor, strengthening of cell walls, and modulation of defense-hormonal signal networks [26]. Significant up-regulation of DEGs encoding ascorbic acid (ASC) and glutathione (GSH) were also detected in the generated data (Figure S2), suggesting that the ASC and GSH systems may be induced as part of a transduction pathway that triggers defense responses and sequential cell death. Calmodulin (CaM) plays a significant role in sensing and transducing changes in cellular Ca^{2+} concentration in response to several biotic and abiotic stresses [27]. During the interaction between *C. morifolium* and *A. alternata*, a series of defensive signals were also activated, including DEGs encoding CaM/CMLs, which were significantly up regulated. In addition, the chitinase can hydrolyze the chitin component of the pathogen cell wall and release elicitors for defense responses [28]. Activities of the two chitinases in infected chrysanthemum leaves was significantly higher than in control leaves, highlighting their importance in defending against *A. alternata* in *C. morifolium*.

Plant hormones play important roles in regulating developmental processes and signaling networks involved in the plant's response to a wide range of biotic and abiotic stresses [29]. ET signaling components, such as EIN2, EIN3, EBF1/2, ERF1/2, are involved in the regulation of cell death and defense responses [30]. JA signaling is systemically activated in response to various biotic and abiotic stresses, increasing the resistance of host plants to some pathogens [31]. SA also plays an important role in resistance and defense induction in response to pathogen attacks [32]. In this study, more than twenty DEGs involved in ET, JA, and SA metabolism were significantly up-regulated at 24 HPI. Their interplay induced defense responses to *A. alternata* infection. In the present study, several DEGs associated with ABA and BR signaling were up-regulated in the chrysanthemum response to *A. alternata* infection, suggesting that BRs and ABA could be participants in this regulatory response. The participation and characteristics of DGEs in complex phytohormone signaling pathways indicate that these signals are not only simple linear and isolated cascades, but that they also cooperated with one another in response to *A. alternata* infection.

Most importantly, chrysanthemum developed a series of immunity responses when inoculated with *A. alternata*, during which time the pathogen secreted effectors to suppress the host plant's immunity response. Several *A. alternata* genes, beneficial to the pathogen's infection and colonization were also significantly induced during infecting chrysanthemum leaves. The tangerine pathotype of *A. alternata* produces host-selective ACT-toxin, the biosynthesis of which is essentially encoded by a polyketide

synthase gene that is also required for pathogenicity of this fungus [33]. NRPS and cytochrome P450 protein TES1 are required for tentoxin (TEN) biosynthesis in *A. alternata* strain ZJ33 [34], while the PKS gene *ACRTS2* is responsible for host-selective ACR-Toxin biosynthesis in the rough lemon pathotype of *A. alternata* [35]. In the present study, DEGs corresponding to NPRS and PKS homologs were also identified, confirming the importance of this toxin synthesis during *A. alternata* invasion into chrysanthemum. Several studies had also demonstrated that effector proteins can affect plant immune mechanisms by regulating plant gene transcription [36], affecting the secretion of and degrading plant immune-related proteins [37-40], affecting the connection of host cell walls and cell membranes [41, 42], and by regulating plant hormone synthesis and related signaling pathways [43-45]. Extracellular degrading enzymes produced by plant pathogenic fungi are important types of fungal effectors [46]. Our research revealed that a series of degrading enzyme gene homologs were up-regulated, which may be investigated in the future to elucidate the pathogenic mechanism of *A. alternata*.

In order to further determine the interaction mechanism between *C. morifolium* and *A. alternata* during the different (early, middle, and late) infection stages, WGCNA and correlation coefficient analysis were carried out. A series of highly correlated modules between *C. morifolium* and *A. alternata* were identified. PRGdb is a bioinformatics platform for plant resistance gene analysis [24], and PHI-base contains molecular and biological information on genes that have been proven to affect the outcome of pathogen-host interactions [25]. The regulatory network of key genes annotated in PRGdb or PHI-base at the three infection stages were visualized using the Cytoscape software. For example, the regulatory networks of two RGA1-like disease resistance protein homologs were identified at the late infection stage. The ACL1, ACL2, and BUF1 homologs were also identified, which were predicted to influence the virulence of *A. alternata*. Transcription factors are important players in the response to pathogen invasion [47, 48]. The regulatory network of two transcription factors (*CL14283.Contig1_All* and *Unigene25854_All*) were also identified, which may play important roles in response to *A. alternata* infection in *C. morifolium*. Moreover, using the correlation coefficient between key genes of *C. morifolium* and *A. alternata*, highly correlated genes were identified, reinforcing our understanding of the interplay between the two species.

Currently, the interaction mechanism between chrysanthemum and *A. alternata* is not fully understood, and the function of effector proteins from *A. alternata* are unknown too. The discovery of *A. alternata* toxin synthesis genes and candidate effectors will not only improve our understanding of *A. alternata* pathogenesis, but also, perhaps more significantly, provide valuable resources for subsequent investigations into plant-pathogen interactions. The present study has designed a powerful methodology for mixed transcriptome analysis of host plant and pathogen, which has established a foundation for comprehensive research on the pathogenesis of chrysanthemum black spot disease.

Conclusions

In the study, *A. alternata*, chrysanthemum leaves and chrysanthemum leaves infected with *A. alternata* at three infection stages, i.e., the early (no lesion formation), middle (lesion formation) and late (lesion expansion) infection stages were sampled for dual RNA-seq. A total of 153,532 and 14,932 DEGs were

identified in chrysanthemum and *A. alternata*, respectively. Chrysanthemum employed multiple pathways to jointly regulate and respond to pathogenic stress. *A. alternata* induced a variety of metabolic activities during infection, that generated energy and toxic metabolites to attack host cells. The discovery of *A. alternata* toxin synthesis genes and candidate effectors will not only improve our understanding of *A. alternata* pathogenesis, but also, perhaps more significantly, provide valuable resources for subsequent investigations into plant-pathogen interactions. Meanwhile, WGCNA and correlation coefficient analysis were carried out to identify the regulatory network of key genes from highly correlated modules at the three infection stages. Coefficient analyses showed that a number of genes were highly correlated between *C. morifolium* and *A. alternata* at the late infection stage, which provide a broader understanding of the interaction mechanisms between two species. This work gains insights into the interaction between *C. morifolium* and *A. alternata* and elucidate the potential pathogenesis of *A. alternata*, as well as the defense mechanism of *C. morifolium*, which would benefit in inhibiting fungal pathogenicity or breed resistant chrysanthemum cultivars.

Methods

Plant materials and *A. alternata* culture

Chrysanthemum variety ‘Dayangju’ was obtained from the Chrysanthemum Germplasm Resource Preserving Centre of Nanjing Agricultural University, China. Rooting seedlings of approximately similar growth were transplanted into a mixed matrix of 3:1 vermiculite and perlite without add fertilizer. Growth was under 16-h photoperiod, day and night temperatures set to 25 ℃ and 22 ℃, respectively, and relative humidity maintained at 68–75% [1, 2]. The test strain *A. alternata* was isolated and identified from leaves of 'Fubaiju', a variety found in the chrysanthemum tea producing area of Futianhe Town, Macheng City, Hubei Province, China. The test strain was transferred to plates containing PDA (Potato Dextrose Agar) solid medium on a sterile bench and cultured at 25 ℃.

A. alternata inoculation and sampling

The *A. alternata* strain was cultured in flasks containing 200 mL PDW liquid medium on a rotary shaker maintained at 200 revolutions per min, for 24 h. Three groups of fungal suspension were prepared for inoculating and sampling at different time points. Each tested leaf was inoculated with *A. alternata* at four points, and the area of inoculation at each point was designated as consistently as possible. The treatment and control groups were cultured in a cubator maintained at 28 ℃ and 90% humidity in the dark. Once the inoculated leaves reached 1, 12, and 24 hours post inoculation (HPI), representing the three infection stages, the groups were sampled simultaneously. The inoculated parts of leaves (including the fungus) were sampled using a punch and leaves of the control group (without fungus) were similarly sampled in corresponding areas. During chrysanthemum sampling at the three time points, *A. alternata* mycelium was simultaneously sampled on a clean bench. Samples of inoculated and control chrysanthemum leaves, as well as *A. alternata* mycelium were all collected in three replicates, frozen in liquid nitrogen and stored at –80 ° C for dual RNA-seq.

RNA extraction, library construction, and sequencing

Total RNA was isolated from each sample using the RNA-iso Plus reagent (TaKaRa Bio, Tokyo, Japan) following the manufacturer's protocol. In order to assess the integrity, the concentration was tested using a Nano Drop spectrophotometer (Thermo Fisher Scientific, Waltham, MA, USA), and the quality was tested using the Agilent 2100 Bio analyzer (Agilent Technologies, Santa Clara, CA, USA) to include RIN value, 28S/18S ratio, and fragment length distribution. mRNA was enriched using magnetic beads with Oligo (dT); the RNA was fragmented, and reverse-transcribed to double-stranded cDNA (dscDNA) using N6 random primers. The synthesized cDNA was subjected to end-repair followed by 3' adenylation, and adaptors were ligated to the ends of these 3' adenylated cDNA fragments. The ligation products were purified and PCR amplification was performed to enrich the purified cDNA template, using PCR primers. Lastly, the amplicons were denatured by heat and single-stranded DNA was cyclized using splint oligos and DNA ligase. The generated libraries were then used for sequencing on the BGISEQ-500 (BGI) platform, and the products labelled as 'raw reads' [49]. Twenty-seven sets of original readings were obtained, corresponding to control chrysanthemum leaf samples (CK1h CK12h, CK24h; hereafter named the 'CK' sample series), *C. morifolium* leaves infected with *A. alternata* (In1h, In12h, In24h; hereafter named the 'In' sample series), *A. alternata* (Aa1h, Aa12h, Aa24h; hereafter named the 'Aa' sample series), and with three replicates per sample.

De novo assembly and functional annotation

As the reference genome of chrysanthemum was unpublished, we performed de novo assembly in order to reconstruct the transcriptome. Firstly, all generated raw sequencing reads were filtered using the SOAPnuke software (BGI), to remove low quality reads, including adaptor sequences, low quality sequences (where the percentage of low quality bases with a value ≤ 10 was more than 20% in one read), and unknown nucleotides (where unknown bases were more than 5%), and obtain clean reads. Secondly, clean reads with overlap joints were combined to form longer fragments, i.e., contigs. Finally, clean reads were assembled using Trinity, and transcripts were clustered using TGICL, to remove redundancy and obtain unigenes for functional annotation. In the case of multiple samples, TGICL was used again to perform clustering on each sample's unigenes to remove redundancy and obtain the final unigenes for subsequent analysis [50]. Clean reads were aligned to a reference gene sequence using Bowtie2, and the expression level of the unigenes was calculated via the FPKM (fragments per kilobase of transcript per million fragments mapped) method [51]. DEGs were defined according to a threshold of Q-values ≤ 0.001 [52] and an absolute $\log_2$ ratio value ≥ 1, among the three biological replicates. Sequences were compared with the NR (ftp://ftp.ncbi.nlm.nih.gov/blast/db), NT (ftp://ftp.ncbi.nlm.nih.gov/blast/db), Swiss-Prot (www.uniprot.org), Pfam (http://pfam.xfam.org), KEGG (http://www.genome.jp/kegg), KOG (https://www.ncbi.nlm.nih.gov/COG/), and GO (http://geneontology.org) databases, inorder to identify and annotate the generated DEGs [53, 54]. GO categories were assigned to all genes via a BLASTX hit using the Blast2GO software. KEGG was used to map sequences to pathways, and the KOBAS [55] software was used to test the statistical enrichment of DEGs identified in the KEGG pathways. Functions with a Q-value ≤ 0.05 were generally considered to be significantly enriched. Transcription factor

prediction was determined by using getorf (http://emboss.sourceforge.net/apps/cvs/emboss/apps/getorf.html) to find each DEG's ORF, which was then aligned to TF domains (from PlntfDB) using hmmsearch (http://hmmer.org) [56]. As the *A. alternata* genome was published, clean reads (obtained as described above) were aligned to reference genome sequences (https://www.ncbi.nlm.nih.gov/genome/11201?genome_assembly_id=275364) by hierarchical indexing for spliced alignment of transcripts in the HISAT (Hierarchical Indexing for Spliced Alignment of Transcripts) application [57]. *A. alternata* DEGs were identified using a method similar to that described for chrysanthemum. The DIAMOND software (https://github.com/bbuchfink/diamond) was used to annotate the DEG comparison to the PHI-base (Pathogen Host Interaction Database), and annotation results were further screened based on conditions where query coverage ≥ 50% and identity ≥ 40%, in order to find potentially pathogenic genes in *A. alternata*. At the same time, GO classification and KEGG pathway enrichment were also performed [58].

Weighted gene co-expression network analysis

Weighted gene co-expression network analysis (WGCNA) was performed to identify key genes using the WGCNA R package [59]. The adjacency matrix was built based on normalized FPKM values, following which modules containing transcripts with similar expression patterns were created, and key genes for these modules were calculated. Gene significance (value >= 0.8) and connectivity (top 20%) were used to identify hub genes. Co-expression networks were visualized using Cytoscape software[60]. Highly correlated modules and genes were calculated by correlation coefficient and defined according to a threshold of $r \geq 0.8$ and a p-value < 0.05.

qRT-PCR validation and analysis

RNA-seq results were validated by selecting 12 DEGs to examine the consistency of their expression profiles. Total RNA (1 mg) was reverse-transcribed using the Prime Script™ RT Master Mix (Perfect Real Time) (Takara) following the manufacturer's instructions. Gene-specific primers for quantitative real-time PCR (qRT-PCR) analysis were designed using the Primer 5.0 software. The chrysanthemum *CmEF1α* gene was used as a reference, and gene primers are listed in Table S1. Three biological replicates were performed per sample, and qRT-PCR was performed as previously described by Li et al. [1]. The relative expression level of each sample was calculated using the $2^{-\Delta\Delta CT}$ method [61].

Declarations

Author contributions

LY and GZY designed the experiment. LY and LLN performed the experiment. LY and LLN analyzed the data. LY, GZY and LLN wrote the manuscript. LY and GZY revised the manuscript. All authors read and approved the final manuscript.

Acknowledgements

This work was funded by the National Key Research and Development Program of China (2018YFD1000400), the Jiangsu Modern Industrial System Project (130601169, 130601172), A project Funded by the Priority Academic Program Development of Jiangsu Higher Education Institution, the Natural Science Fund of Qinghai Province, China (2018-HZ-819), and the National Natural Science Foundation of China (31700620).

Competing interests

The authors declare that have no conflict of interests.

References

1. Li H, Chen S, Song A, Wang H, Fang W, Guan Z, Jiang J, Chen F: **RNA-Seq derived identification of differential transcription in the chrysanthemum leaf following inoculation with Alternaria tenuissima**. *BMC Genomics* 2014, **15**:9.
2. Liu Y, Xin J, Liu L, Song A, Guan Z, Fang W, Chen F: **A temporal gene expression map of Chrysanthemum leaves infected with Alternaria alternata reveals different stages of defense mechanisms**. *Hortic Res* 2020, **7**:23.
3. N VDB, Berger DK, Hein I, Birch PR, Wingfield MJ, Viljoen A: **Tolerance in banana to Fusarium wilt is associated with early up-regulation of cell wall-strengthening genes in the roots**. *Mol Plant Pathol* 2007, **8**(3):333-341.
4. Makkar HP, Siddhuraju P, Becker K: **Plant secondary metabolites**. *Methods Mol Biol* 2007, **393**:1-122.
5. Berrocal-Lobo M, Molina A: **Arabidopsis defense response against Fusarium oxysporum**. *Trends Plant Sci* 2008, **13**(3):145-150.
6. Zhu L, Ni W, Liu S, Cai B, Xing H, Wang S: **Transcriptomics Analysis of Apple Leaves in Response to Alternaria alternata Apple Pathotype Infection**. *Front Plant Sci* 2017, **8**:22.
7. He Y, Jia R, Qi J, Chen S, Lei T, Xu L, Peng A, Yao L, Long Q, Li Z *et al*: **Functional analysis of citrus AP2 transcription factors identified CsAP2-09 involved in citrus canker disease response and tolerance**. *Gene* 2019, **707**:178-188.
8. Xu W, Ma F, Li R, Zhou Q, Yao W, Jiao Y, Zhang C, Zhang J, Wang X, Xu Y *et al*: **VpSTS29/STS2 enhances fungal tolerance in grapevine through a positive feedback loop**. *Plant Cell Environ* 2019, **42**(11):2979-2998.
9. Yang X, Hu H, Yu D, Sun Z, He X, Zhang J, Chen Q, Tian R, Fan J: **Candidate Resistant Genes of Sand Pear (Pyrus pyrifolia Nakai) to Alternaria alternata Revealed by Transcriptome Sequencing**. *PLoS One* 2015, **10**(8):e0135046.
10. Song W, Qi N, Liang C, Duan F, Zhao H: **Soybean root transcriptome profiling reveals a nonhost resistant response during Heterodera glycines infection**. *PLoS One* 2019, **14**(5):e0217130.
11. Milc J, Bagnaresi P, Aragona M, Valente MT, Biselli C, Infantino A, Francia E, Pecchioni N: **Comparative transcriptome profiling of the response to Pyrenochaeta lycopersici in resistant tomato**

cultivar Mogeor and its background genotype-susceptible Moneymaker. *Funct Integr Genomics* 2019, **19**(5):811-826.

12. Westermann AJ, Gorski SA, Vogel J: **Dual RNA-seq of pathogen and host**. *Nat Rev Microbiol* 2012, **10**(9):618-630.
13. Naidoo S, Visser EA, Zwart L, Toit YD, Bhadauria V, Shuey LS: **Dual RNA-Sequencing to Elucidate the Plant-Pathogen Duel**. *Curr Issues Mol Biol* 2018, **27**:127-142.
14. Burgess DJ: **Gene expression: Host-pathogen duels revealed by dual RNA-seq in vivo**. *Nat Rev Genet* 2017, **18**(3):143.
15. Pieterse CM, Leon-Reyes A, Van der Ent S, Van Wees SC: **Networking by small-molecule hormones in plant immunity**. *Nat Chem Biol* 2009, **5**(5):308-316.
16. Wang ZY: **Brassinosteroids modulate plant immunity at multiple levels**. *Proc Natl Acad Sci U S A* 2012, **109**(1):7-8.
17. Pavon Moreno MA, Gonzalez Alonso I, Martin de Santos R, Garcia Lacarra T: **The importance of genus Alternaria in mycotoxins production and human diseases**. *Nutr Hosp* 2012, **27**(6):1772-1781.
18. Hou Y, Ma X, Wan W, Long N, Zhang J, Tan Y, Duan S, Zeng Y, Dong Y: **Comparative Genomics of Pathogens Causing Brown Spot Disease of Tobacco: Alternaria longipes and Alternaria alternata**. *PLoS One* 2016, **11**(5):e0155258.
19. Saha D, Fetzner R, Burkhardt B, Podlech J, Metzler M, Dang H, Lawrence C, Fischer R: **Identification of a polyketide synthase required for alternariol (AOH) and alternariol-9-methyl ether (AME) formation in Alternaria alternata**. *PLoS One* 2012, **7**(7):e40564.
20. Cantarel BL, Coutinho PM, Rancurel C, Bernard T, Lombard V, Henrissat B: **The Carbohydrate-Active EnZymes database (CAZy): an expert resource for Glycogenomics**. *Nucleic Acids Res* 2009, **37**(Database issue):D233-238.
21. Huckelhoven R: **Cell wall-associated mechanisms of disease resistance and susceptibility**. *Annu Rev Phytopathol* 2007, **45**:101-127.
22. Li F, Wu X, Lam P, Bird D, Zheng H, Samuels L, Jetter R, Kunst L: **Identification of the wax ester synthase/acyl-coenzyme A: diacylglycerol acyltransferase WSD1 required for stem wax ester biosynthesis in Arabidopsis**. *Plant Physiol* 2008, **148**(1):97-107.
23. Kurdyukov S, Faust A, Trenkamp S, Bar S, Franke R, Efremova N, Tietjen K, Schreiber L, Saedler H, Yephremov A: **Genetic and biochemical evidence for involvement of HOTHEAD in the biosynthesis of long-chain alpha-,omega-dicarboxylic fatty acids and formation of extracellular matrix**. *Planta* 2006, **224**(2):315-329.
24. Osuna-Cruz CM, Paytuvi-Gallart A, Di Donato A, Sundesha V, Andolfo G, Aiese Cigliano R, Sanseverino W, Ercolano MR: **PRGdb 3.0: a comprehensive platform for prediction and analysis of plant disease resistance genes**. *Nucleic Acids Res* 2018, **46**(D1):D1197-D1201.
25. Urban M, Cuzick A, Seager J, Wood V, Rutherford K, Venkatesh SY, De Silva N, Martinez MC, Pedro H, Yates AD *et al*: **PHI-base: the pathogen-host interactions database**. *Nucleic Acids Res* 2020, **48**(D1):D613-D620.

26. Mauch-Mani B, Mauch F: **The role of abscisic acid in plant-pathogen interactions**. *Curr Opin Plant Biol* 2005, **8**(4):409-414.
27. Ali GS, Reddy VS, Lindgren PB, Jakobek JL, Reddy AS: **Differential expression of genes encoding calmodulin-binding proteins in response to bacterial pathogens and inducers of defense responses**. *Plant Mol Biol* 2003, **51**(6):803-815.
28. Kesari P, Patil DN, Kumar P, Tomar S, Sharma AK, Kumar P: **Structural and functional evolution of chitinase-like proteins from plants**. *Proteomics* 2015, **15**(10):1693-1705.
29. Bari R, Jones JD: **Role of plant hormones in plant defence responses**. *Plant Mol Biol* 2009, **69**(4):473-488.
30. Bouchez O, Huard C, Lorrain S, Roby D, Balague C: **Ethylene is one of the key elements for cell death and defense response control in the Arabidopsis lesion mimic mutant vad1**. *Plant Physiol* 2007, **145**(2):465-477.
31. Turner JG, Ellis C, Devoto A: **The jasmonate signal pathway**. *Plant Cell* 2002, **14 Suppl**:S153-164.
32. Robert-Seilaniantz A, Grant M, Jones JD: **Hormone crosstalk in plant disease and defense: more than just jasmonate-salicylate antagonism**. *Annu Rev Phytopathol* 2011, **49**:317-343.
33. Miyamoto Y, Masunaka A, Tsuge T, Yamamoto M, Ohtani K, Fukumoto T, Gomi K, Peever TL, Tada Y, Ichimura K *et al*: **ACTTS3 encoding a polyketide synthase is essential for the biosynthesis of ACT-toxin and pathogenicity in the tangerine pathotype of Alternaria alternata**. *Mol Plant Microbe Interact* 2010, **23**(4):406-414.
34. Li YH, Han WJ, Gui XW, Wei T, Tang SY, Jin JM: **Putative Nonribosomal Peptide Synthetase and Cytochrome P450 Genes Responsible for Tentoxin Biosynthesis in Alternaria alternata ZJ33**. *Toxins (Basel)* 2016, **8**(8).
35. Izumi Y, Ohtani K, Miyamoto Y, Masunaka A, Fukumoto T, Gomi K, Tada Y, Ichimura K, Peever TL, Akimitsu K: **A polyketide synthase gene, ACRTS2, is responsible for biosynthesis of host-selective ACR-toxin in the rough lemon pathotype of Alternaria alternata**. *Mol Plant Microbe Interact* 2012, **25**(11):1419-1429.
36. Zhu W, Yang B, Chittoor JM, Johnson LB, White FF: **AvrXa10 contains an acidic transcriptional activation domain in the functionally conserved C terminus**. *Mol Plant Microbe Interact* 1998, **11**(8):824-832.
37. Nomura K, Mecey C, Lee YN, Imboden LA, Chang JH, He SY: **Effector-triggered immunity blocks pathogen degradation of an immunity-associated vesicle traffic regulator in Arabidopsis**. *Proc Natl Acad Sci U S A* 2011, **108**(26):10774-10779.
38. Song J, Win J, Tian M, Schornack S, Kaschani F, Ilyas M, van der Hoorn RA, Kamoun S: **Apoplastic effectors secreted by two unrelated eukaryotic plant pathogens target the tomato defense protease Rcr3**. *Proc Natl Acad Sci U S A* 2009, **106**(5):1654-1659.
39. Gimenez-Ibanez S, Hann DR, Ntoukakis V, Petutschnig E, Lipka V, Rathjen JP: **AvrPtoB targets the LysM receptor kinase CERK1 to promote bacterial virulence on plants**. *Curr Biol* 2009, **19**(5):423-429.

40. Kim JG, Stork W, Mudgett MB: **Xanthomonas type III effector XopD desumoylates tomato transcription factor SlERF4 to suppress ethylene responses and promote pathogen growth**. *Cell Host Microbe* 2013, **13**(2):143-154.
41. Singh P, Zimmerli L: **Lectin receptor kinases in plant innate immunity**. *Front Plant Sci* 2013, **4**:124.
42. Bouwmeester K, Han M, Blanco-Portales R, Song W, Weide R, Guo LY, van der Vossen EA, Govers F: **The Arabidopsis lectin receptor kinase LecRK-I.9 enhances resistance to Phytophthora infestans in Solanaceous plants**. *Plant Biotechnol J* 2014, **12**(1):10-16.
43. Djamei A, Schipper K, Rabe F, Ghosh A, Vincon V, Kahnt J, Osorio S, Tohge T, Fernie AR, Feussner I *et al*: **Metabolic priming by a secreted fungal effector**. *Nature* 2011, **478**(7369):395-398.
44. Mukhtar MS, Carvunis AR, Dreze M, Epple P, Steinbrenner J, Moore J, Tasan M, Galli M, Hao T, Nishimura MT *et al*: **Independently evolved virulence effectors converge onto hubs in a plant immune system network**. *Science* 2011, **333**(6042):596-601.
45. Cui H, Wang Y, Xue L, Chu J, Yan C, Fu J, Chen M, Innes RW, Zhou JM: **Pseudomonas syringae effector protein AvrB perturbs Arabidopsis hormone signaling by activating MAP kinase 4**. *Cell Host Microbe* 2010, **7**(2):164-175.
46. Hogenhout SA, Van der Hoorn RA, Terauchi R, Kamoun S: **Emerging concepts in effector biology of plant-associated organisms**. *Mol Plant Microbe Interact* 2009, **22**(2):115-122.
47. Amorim LLB, da Fonseca Dos Santos R, Neto JPB, Guida-Santos M, Crovella S, Benko-Iseppon AM: **Transcription Factors Involved in Plant Resistance to Pathogens**. *Curr Protein Pept Sci* 2017, **18**(4):335-351.
48. Singh K, Foley RC, Onate-Sanchez L: **Transcription factors in plant defense and stress responses**. *Curr Opin Plant Biol* 2002, **5**(5):430-436.
49. Li J, Gao Z, Zhou L, Li L, Zhang J, Liu Y, Chen H: **Comparative transcriptome analysis reveals K(+) transporter gene contributing to salt tolerance in eggplant**. *BMC Plant Biol* 2019, **19**(1):67.
50. Jiang SH, Sun QG, Chen M, Wang N, Xu HF, Fang HC, Wang YC, Zhang ZY, Chen XS: **Methylome and transcriptome analyses of apple fruit somatic mutations reveal the difference of red phenotype**. *BMC Genomics* 2019, **20**(1):117.
51. Conesa A, Gotz S, Garcia-Gomez JM, Terol J, Talon M, Robles M: **Blast2GO: a universal tool for annotation, visualization and analysis in functional genomics research**. *Bioinformatics* 2005, **21**(18):3674-3676.
52. Storey JD, Tibshirani R: **Statistical significance for genomewide studies**. *Proc Natl Acad Sci U S A* 2003, **100**(16):9440-9445.
53. Pruitt KD, Tatusova T, Maglott DR: **NCBI reference sequences (RefSeq): a curated non-redundant sequence database of genomes, transcripts and proteins**. *Nucleic Acids Res* 2007, **35**(Database issue):D61-65.
54. Altschul SF, Madden TL, Schaffer AA, Zhang J, Zhang Z, Miller W, Lipman DJ: **Gapped BLAST and PSI-BLAST: a new generation of protein database search programs**. *Nucleic Acids Res* 1997, **25**(17):3389-3402.

55. Mao X, Cai T, Olyarchuk JG, Wei L: **Automated genome annotation and pathway identification using the KEGG Orthology (KO) as a controlled vocabulary**. *Bioinformatics* 2005, **21**(19):3787-3793.
56. Mistry J, Finn RD, Eddy SR, Bateman A, Punta M: **Challenges in homology search: HMMER3 and convergent evolution of coiled-coil regions**. *Nucleic Acids Res* 2013, **41**(12):e121.
57. Kim D, Langmead B, Salzberg SL: **HISAT: a fast spliced aligner with low memory requirements**. *Nat Methods* 2015, **12**(4):357-360.
58. Buchfink B, Xie C, Huson DH: **Fast and sensitive protein alignment using DIAMOND**. *Nat Methods* 2015, **12**(1):59-60.
59. Zhang B, Horvath S: **A general framework for weighted gene co-expression network analysis**. *Stat Appl Genet Mol Biol* 2005, **4**:Article17.
60. Stuart JM, Segal E, Koller D, Kim SK: **A gene-coexpression network for global discovery of conserved genetic modules**. *Science* 2003, **302**(5643):249-255.
61. Livak KJ, Schmittgen TD: **Analysis of relative gene expression data using real-time quantitative PCR and the 2(-Delta Delta C(T)) Method**. *Methods* 2001, **25**(4):402-408.

Figures

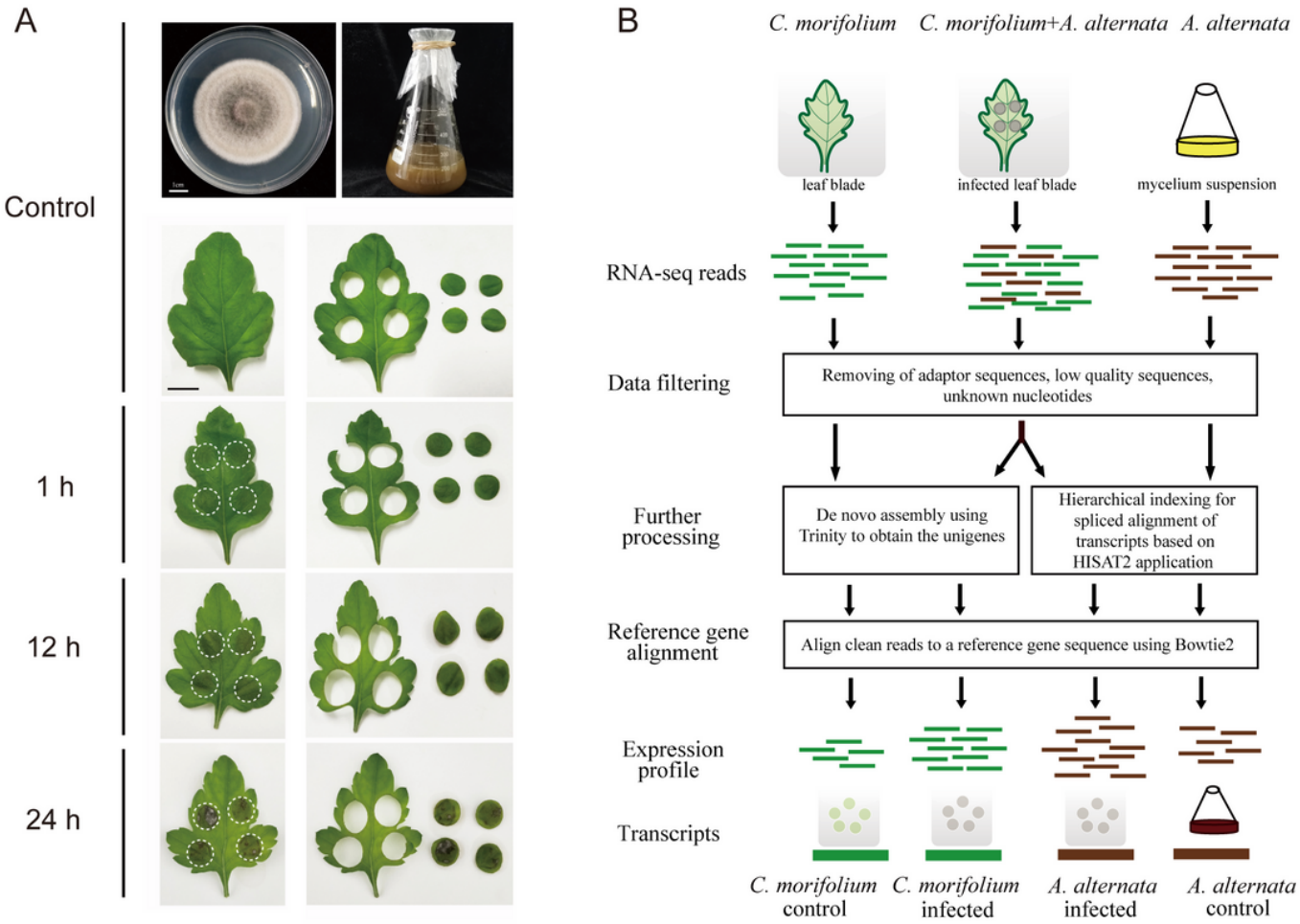

Figure 1

Inoculating, sampling, a 2 nd dual RNA-seq analysis process. (A) Morphology of A. alternata, healthy chrysanthemum leaves, and A. alternata inoculated chrysanthemum leaves. Image showing leaf spots on the upper side at 1, 12, and 24 HPI. Scale bar = 1 cm; (B) Flow chart representing dual RNA-seq analysis of mixed transcriptome obtained from chrysanthemum leaves infected with A. alternata.

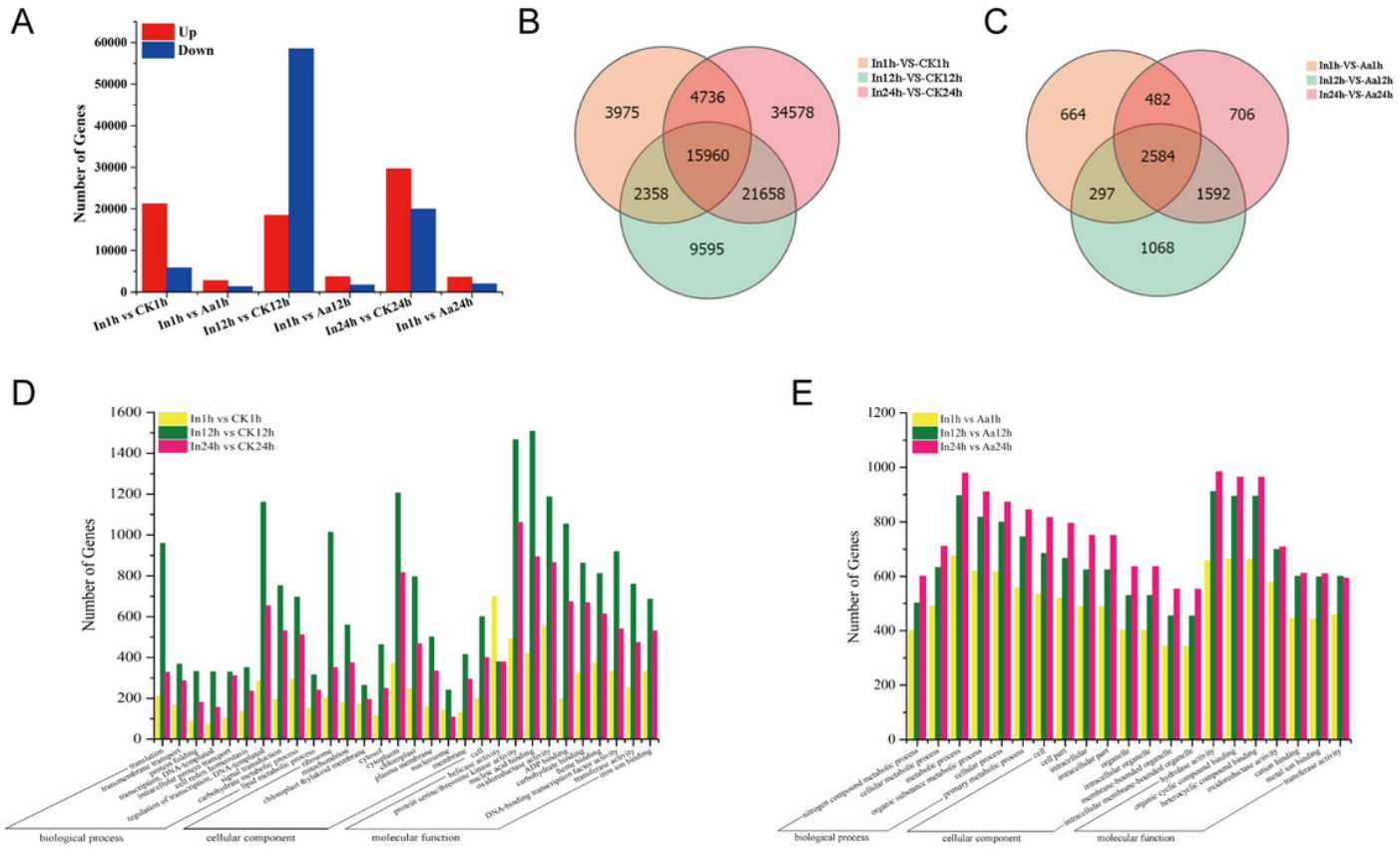

Figure 2

DEGs comparisons between sample types. (A) Number of DEGs compared between two sample types (i.e., In1h vs. CK1h, In1h vs. Aa1h, In12h vs. CK12h, In12h vs. Aa12h, In24h vs. CK24h, and In24h vs. Aa24h). DEGs are shown in red (up-regulated) and blue (down-regulated); (B) Venn diagram representation of unique and shared DEGs between the 'In' and 'Ck' sample series, at the tested time points; (C) V Venn diagram representation of unique and shared DEGs between the 'In' and 'Aa' sample series, at the tested time points; (D) GO functional enrichment analysis of chrysanthemum DEGs; (E) GO functional enrichment analysis of A. alternata DEGs.

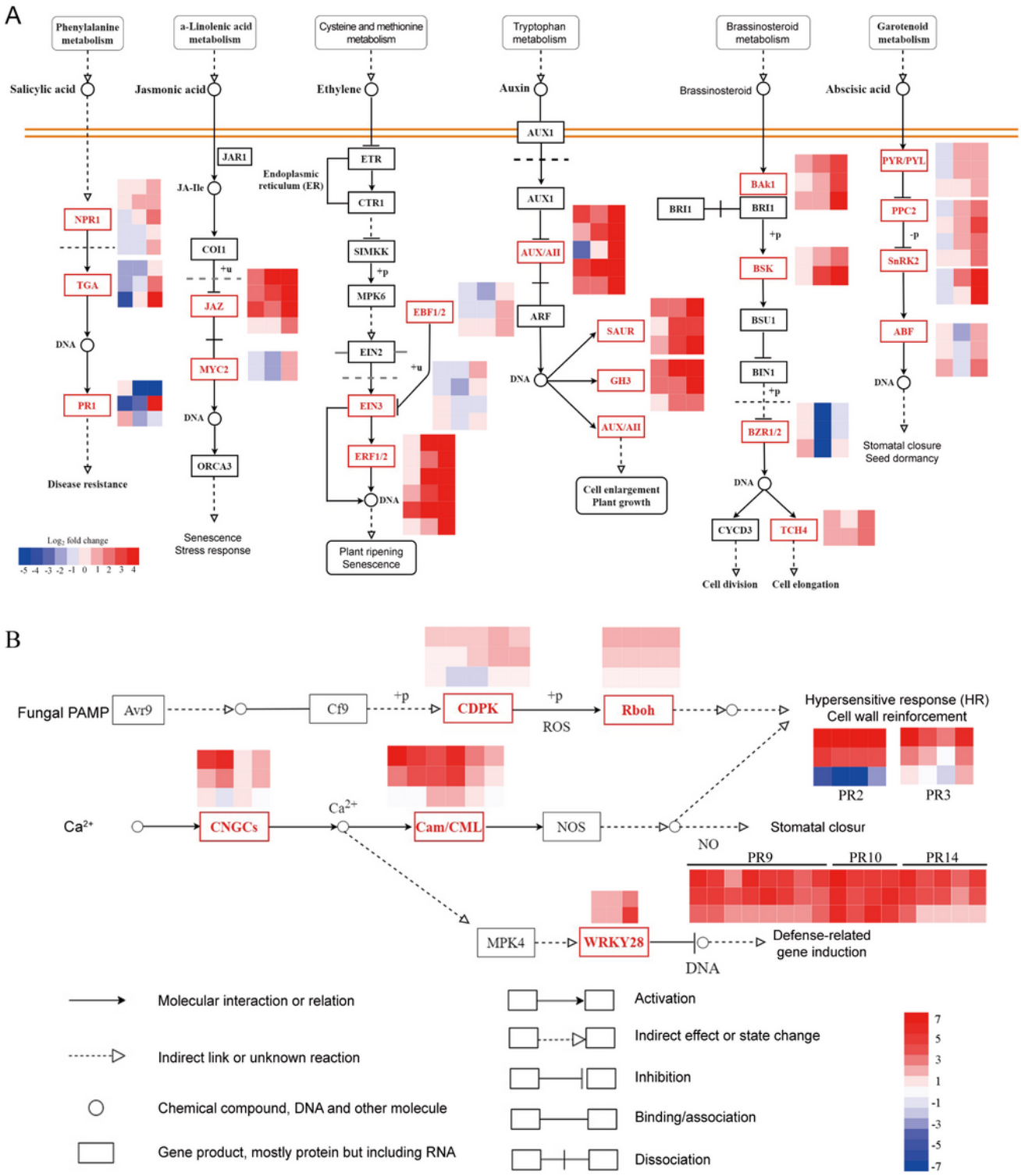

Figure 3

DEGs involved in phytohormone signaling transduction and plant-fungal interaction pathways. (A) DEGs involved in phytohormone signaling transduction pathways. From left to right: salicylic acid (SA), jasmonic acid (JA), ethylene (ET), auxin (AUX), brassinosteroid (BR), and abscisic acid (ABA). Each vertical column represents 1, 12, and 24 HPI from left to right, and each horizontal row represents a DEG; (B) DEGs involved in plant-fungal interactions. Each vertical column represents a DEG and each

horizontal row represents 1, 12, and 24 BPI from bottom to top. Expression values are presented as log, fold-change value (red represents up-regulation; blue represents down-regulation).

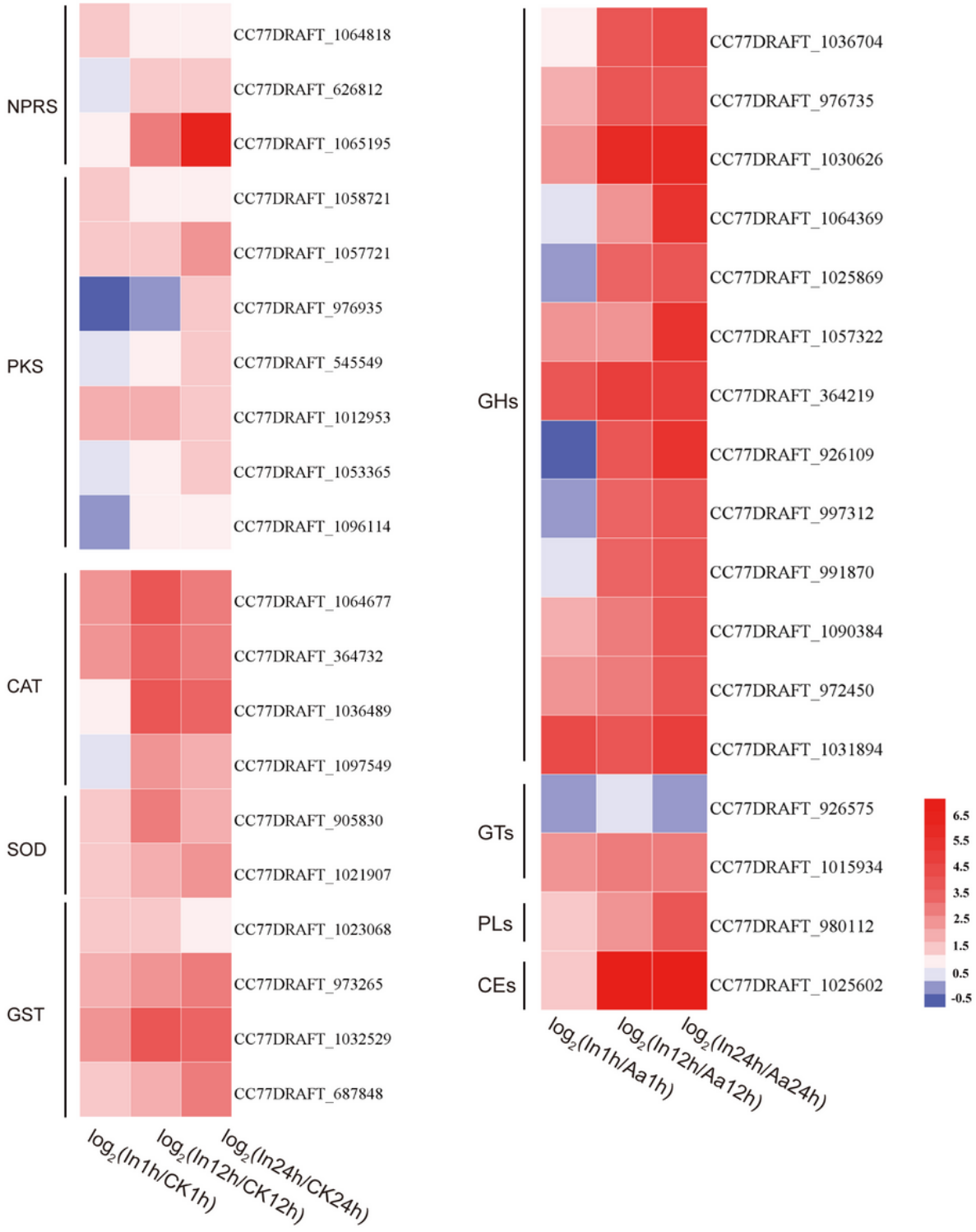

Figure 4

DEGs related to A. alternata virulence.

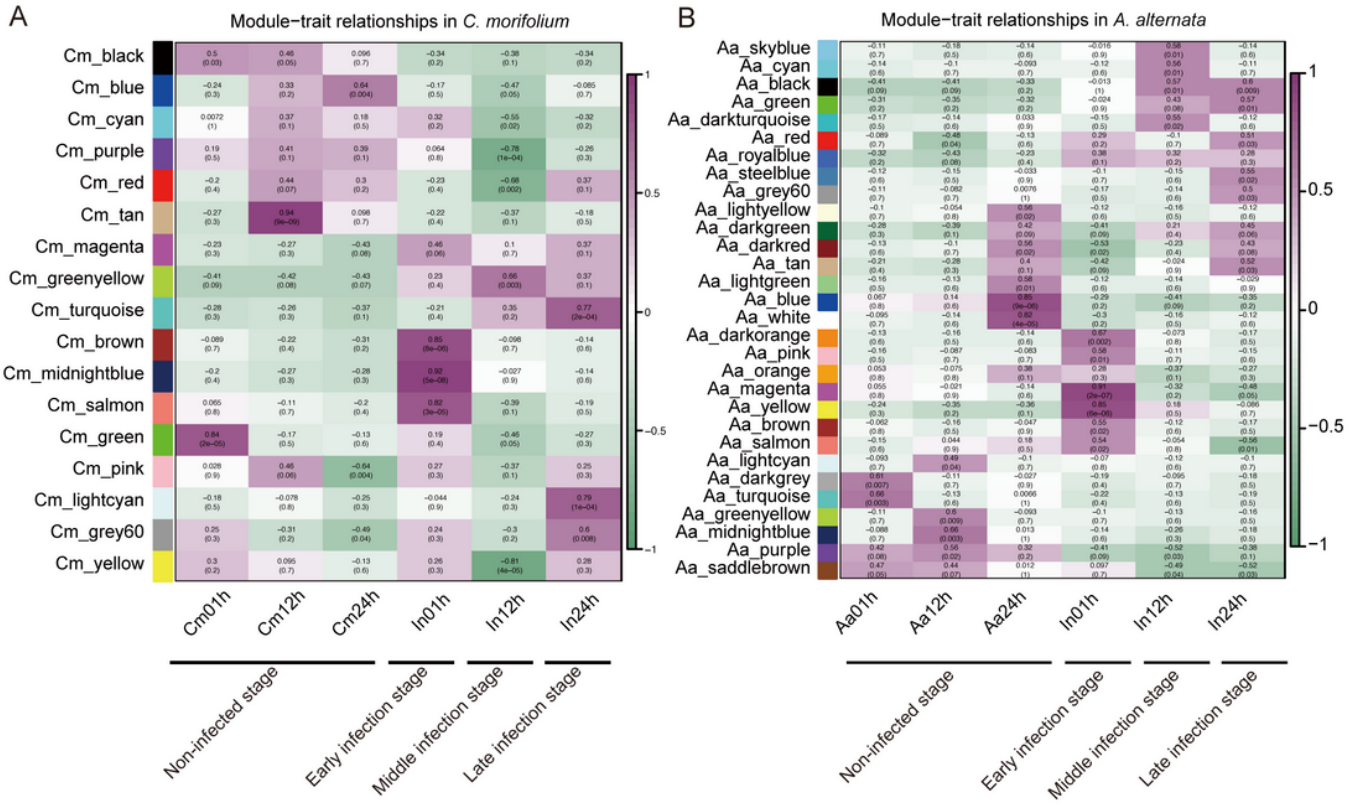

Figure 5

WGCNA results revealed modules highly correlated with phenotype traits in C morifolium (A) and A. alternata (B).

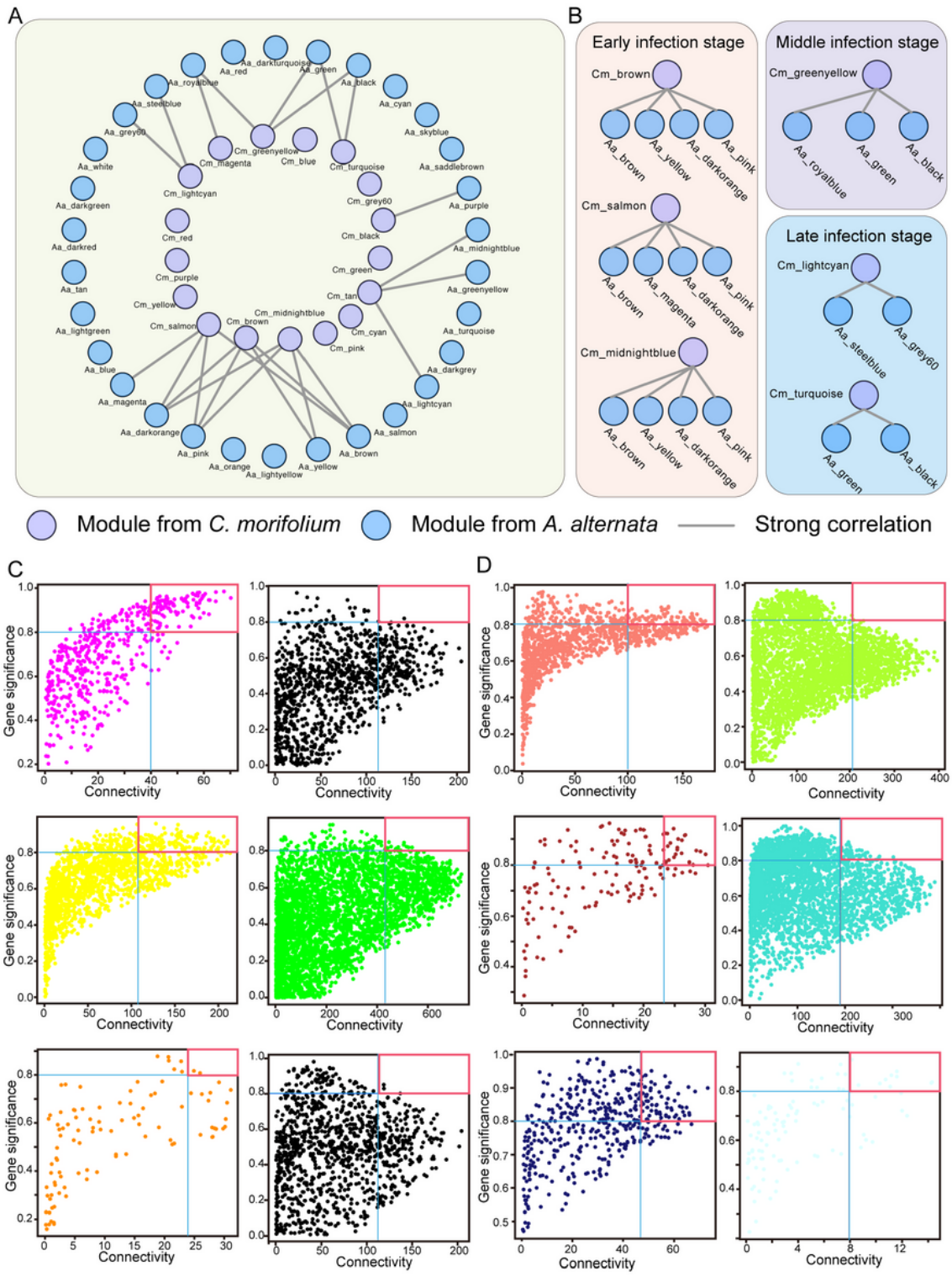

Figure 6

Correlation analysis between modules from C. morifolium and A. alternata. (A) Network of C. morifolium and A. alternata modules. Highly correlated modules (r > 0.8 and p-value < 0.05) are linked by a line; (B) Network of C. morifolium and A. alternata modules at different stages of infection; (C, D) key gene identification in the highly correlated modules of C. morifolium (C) and A. alternata (D).

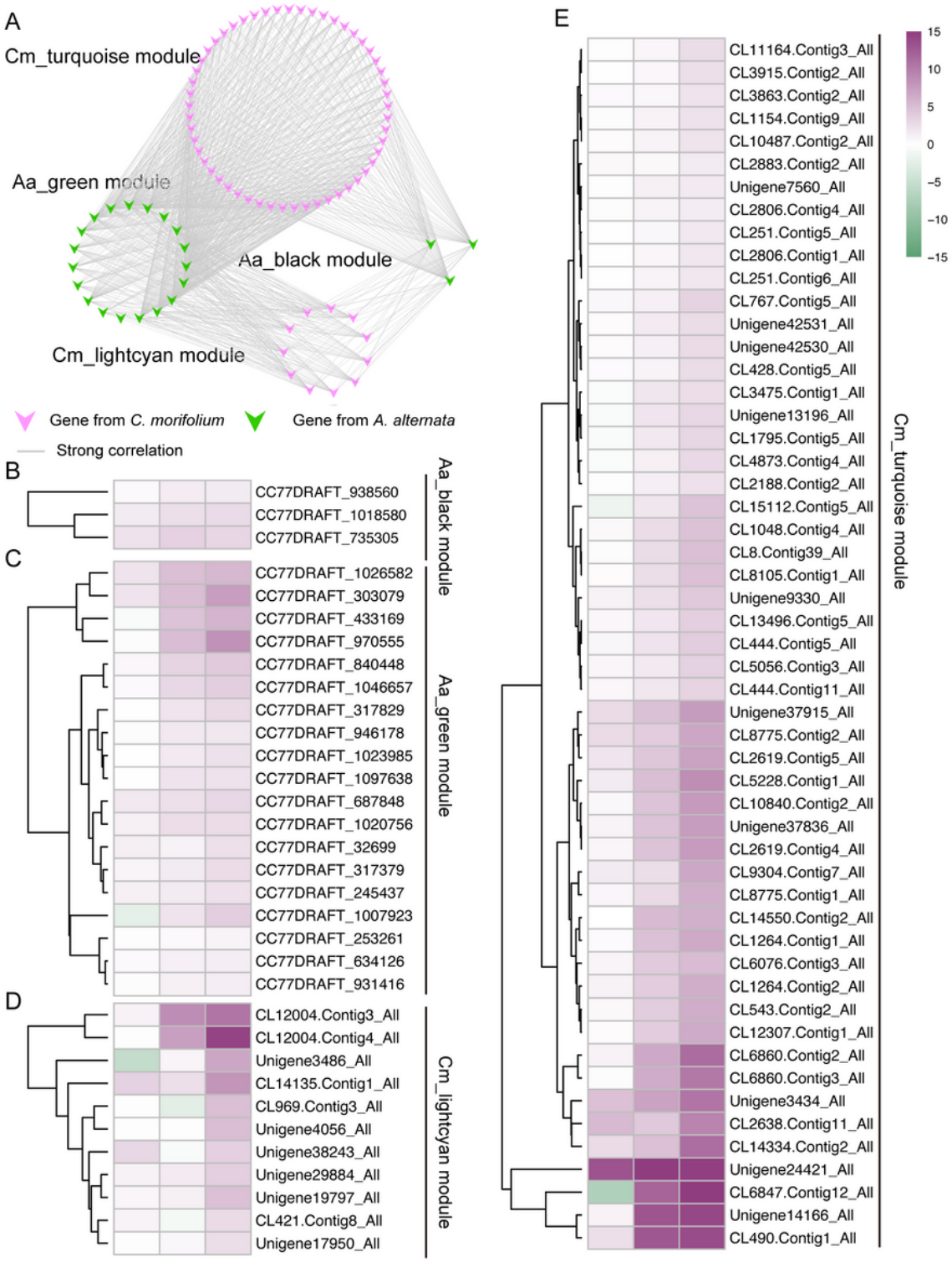

Figure 7

Gene Interplay between C. morifolium and A. alternata at the late infection stage. (A) Network genes from C. morifolium and A. alternata in the late infection stage. Highly correlated genes ($r > 0.8$ and p-value < 0.05) are linked by a line; (B) Heatmap of highly correlated genes from C. morifolium and A. alternate at the late infection stage.

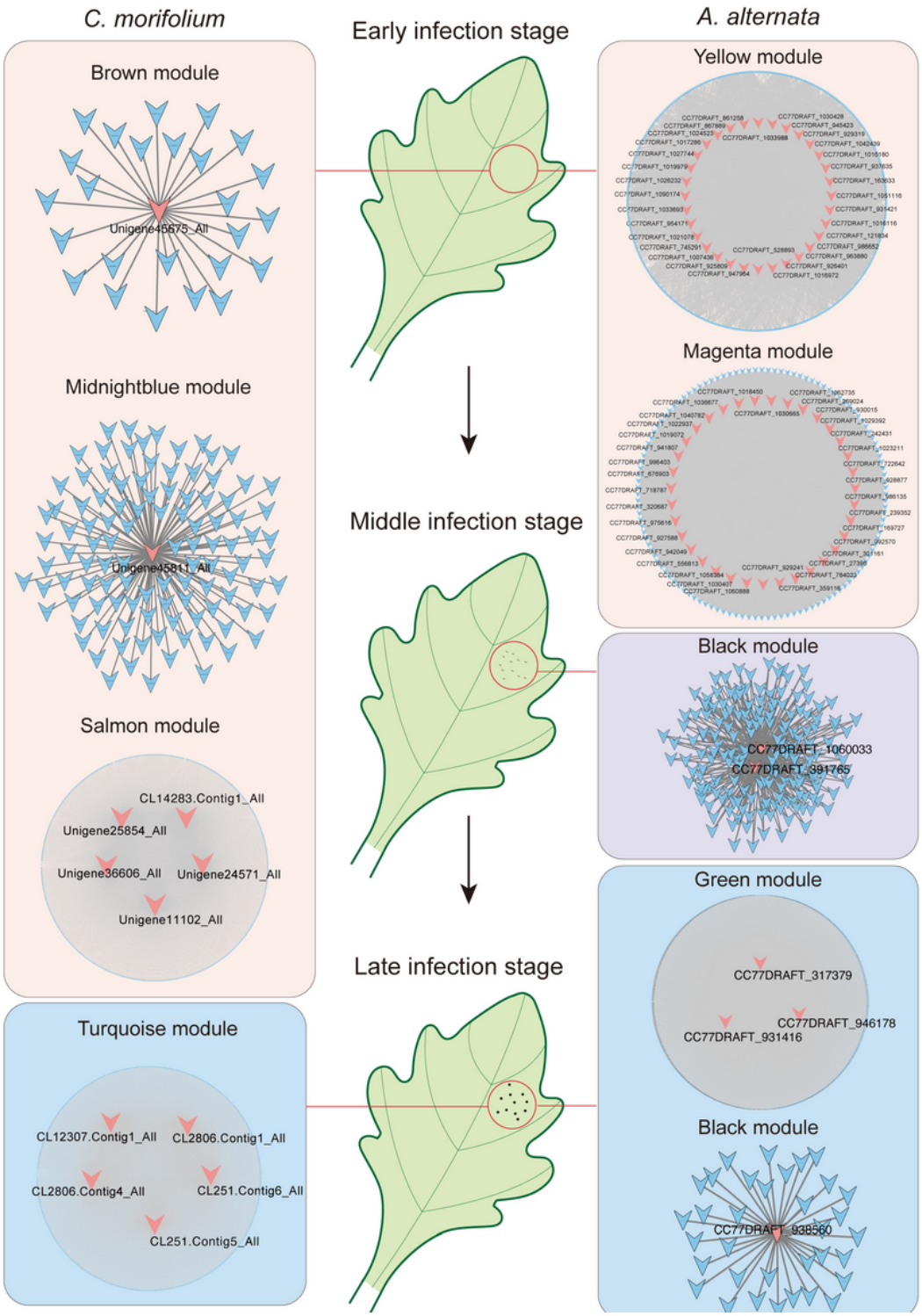

Figure 8

Co-expression networks of key genes from C. morifolium and A. alternata at the three stages of infection.

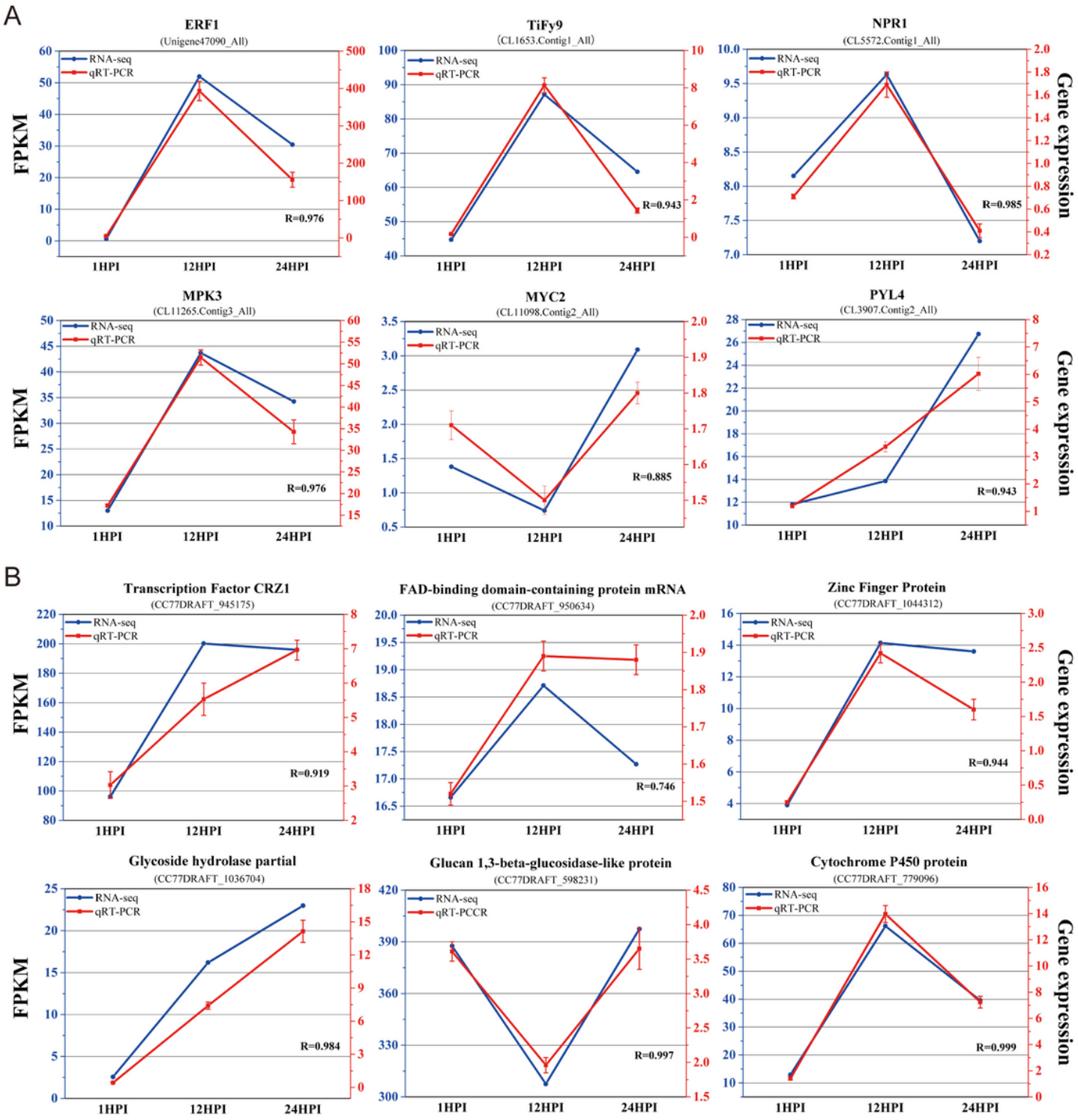

Figure 9

The relative expression level change of DEGs from C. morifolium (A) and A. alternata (B) by RNA-seq and qRT-PCR. Left vertical axis coordinate represents FPKM from RNA-seq (blue); right vertical axis coordinate represents relative gene expression level from qRT-PCR (red). R-values are the relative coefficients between qRT-PCR and RNA-seq.

Supplementary Files

This is a list of supplementary files associated with this preprint. Click to download.

- 04Additionalfiles.pdf